PAK Publishing Group
Growing Knowledge for Future

Proceedings Book of ICETSR, 2014, Malaysia
Handbook on the Emerging Trends in Scientific Research
ISBN: 978-969-9347-16-0

Theoretical Investigation of Both Size and Shape Effects on Ferromagnetic Nanocrystals Curie Temperature

S.N. Hosseinimotlagh
Department of Physics, Shiraz branch Islamic Azad University, Shiraz, Iran
M.Fereshteh
Payame Noor University, Golestan Town, Shiraz
M.Shahamiri
Sama Technical and Vocational College , Islamic Azad University , Kazeroon Branch
Kazeroon, Iran
A.R.Kiani
Nemazee Teaching Hospital. Shiraz University of Medical Sciences. Shiraz, Iran

Abstract

In this paper we study about both size and shape effects on the Transition temperature of ferromagnetic nanocrystals for the first time. Also a thermodynamic approach is proposed to the mechanism of size and shape dependent of ferromagnetic transition temperature. One relation that is obtained, is a simple and unified function without any adjustable parameter that pre-established for the size dependent of ferromagnetic. Also to find of shape effects on the Curie temperature of ferromagnetic nanoparticles a model was developed, that is based on the relation cohesive energy and temperature variations.

1. Introduction

With the miniaturization of devices, size effects become important for the properties of nanomaterial. When the size reduces to nanometers, ferromagnetic solids may exhibit superparamagnetism (TANG, *et al.*, 2004) and lower Curie temperature (EVANS, *et al.*, 2006), (FISHER and BARBER, 1972), (HONG, *et al.*, 2005), (SUN, *et al.*, 2004) and (YANG and JIANG, 2005) T_c of ferromagnetic nanoparticles decrease with decreasing diameter.

Some models have been developed to understand the experimental the observation of T_c suppression. The first one is established in 1972 by FISHER and BARBER that is based on the thickness variation effect on the ferromagnetic transition temperature (Zhang and Willis, 2001). This theory predict that when the spin- spin correlation length beyond from the film thickness, critical temperature shift to a lower temperature Than the bulk value in the thin films .The relation of curie temperature to thickness for thin films is:

$$t(n) = 1 - \frac{T_c(D)}{T_c(\infty)} \approx \left[\frac{(N_0+1)}{2n}\right]^{\lambda} \quad n>N_0 \qquad (1)$$

For ultrathin films:

$$t(n) = 1 - \frac{T_c(D)}{T_c(\infty)} \approx 1 - \frac{n-1}{2N_0} \quad n<N_0 \qquad (2)$$

where D is the size of Nano crystals, $T_c(D)$ denotes the Curie temperature, $T_c(\infty)$ shows the bulk value of Curie temperature, N_0 is the key parameter, the range of the spin-spin coupling and n denotes the film thickness. NIKOLAEV and SHIPILIN (NIKOLAEV and SHIPILIN, 2003) have proposed a $T_c(D)$function in light of the effect of breaking of exchange bond that has been proposed as:

$$\frac{\mathrm{T_{cm}(D)}}{\mathrm{T_{cm}}(\infty)} = 1 - \frac{3\Delta \mathrm{l}}{2\mathrm{D}} \qquad (3a)$$

$$\Delta l \approx \frac{2(\alpha_s - 1)}{3} D_0 \qquad (3b)$$

$$\alpha_s = 1 + \frac{2S_{\mathrm{vib}}}{3R} \qquad (3c)$$

where ΔL is the thickness of the surface layer of nanoparticle. S_{vib} shows the vibrational entropy and R denotes the gas constant. However when this model is utilized to fit experimental data for Fe_2O_3 nanoparticles of different size a constant ΔL is unsuccessful in the full size range of nano size.

To predict the size-dependence of melting temperature, JIANG et al proposed a model that is based on the size dependent cohesive energy function a model for the $T_c(D)$ of Nano crystals

$$\frac{T_C(\mathrm{D})}{T_C(\infty)} = \frac{E(D)}{E(\infty)} \qquad (4)$$

$$\frac{T_C(\mathrm{D})}{T_C(\infty)} = \left[1 - \frac{1}{\left(\frac{2D}{ch} - 1\right)}\right] \exp\left[-\frac{2S_b}{3R}\frac{1}{\left(\frac{2D}{ch} - 1\right)}\right] \qquad (5)$$

where S_b is the bulk evaporation entropy of crystals. D_0 denotes a critical diameter, which related to the atomic or molecular diameter h through. C is added as an additional condition for different surface states. C=1 for low dimensional Material with free surface Where the potential of surface atoms of the Nano crystals differs from the interior Nano crystals. When the interface interaction between the Nano crystals and the corresponding substrates is weak, such as thin films deposited on inert substrates, the film/substrate interaction is of weak Vanderwals forces while the inner interactions within the thin films are strong chemical bonds C = $\frac{1}{2}$ (CUI, *et al*., 2005), (YANG and JIANG, 2005). All these models are important to find the nature of ferromagnetic transition temperature suppression of nanoparticles.

Also another important aspect of particles is the shape of nanoparticles. For a nanoparticle with the same size different shapes lead to different specific surfaces (CAO, *et al*., 2006), (WAUTELET, *et al*., 2003) and (XIE, *et al*., 2004).

At first we study the theory of shape effect on Curie temperature of ferromagnetic Nano crystals. This theory is based on the relation cohesive energy and temperature variations. Then we have plotted graphs to compare the different nanostructures.

Then we discuss about a simple model for size dependent of Curie temperature that based on the Lindeman criterion, Mott's expression and Shi model. We try to prove it's all about relations. Then we compare previous models and the new model with the available experimental data.

1.1. Theory of Shape Effect on Curie Temperature

The Curie temperature can be regarded directly proportional to the cohesive energy (SUN, *et al*., 2004), (YANG and JIANG, 2005,) and (Zhang and Willis, 2001). As an empirical result, we have:

$$\frac{\mathrm{E_n}}{\mathrm{E_b}} = \frac{\mathrm{T_{cn}}}{\mathrm{T_{cb}}} \qquad (5)$$

Where E and T_c denote cohesive energy and Curie temperature. The subscripts n and b are nanoparticle corresponding bulk, respectively. According to Eq. 5 the Curie temperature should have the same size and shape dependence as cohesive energy. To understand the size and shape effects on cohesive energy are developed a size and shape dependent model for the curie temperature of ferromagnetic nanoparticles.

The values of cohesive energy in nanoparticles are different for superficial part and interior part. It is because of their thermal behavior difference. Accordingly the surface to volume atomic ratio dependent expressed as.

$$E_n = (1-\propto)E_b + \propto E_s \tag{6}$$

The subscript's' is the surface. α means the surface to volume atomic ratio. According to the concept of coherent energy and the surface coherent energy by surface atoms, E_s Can be expressed as follows (ADAMSON, 1990,):

$$E_s = (1-\beta)\frac{E_b}{4} + \beta[\frac{E_b}{4} + \frac{3}{4}\left[\left(\frac{E_b}{2}\right) + \eta\left(\frac{E_m}{2}\right)\right] \tag{7}$$

Which β is the ratio of interior area to surface area. The subscript m denotes the embedding matrix, η represents the misfit between nanoparticles and matrix. In a case of incoherent interface between nanoparticles and matrix, η=0; and for a completely coherent interface, η=1.

With the substitution of Eq. 7 in to Eq. 6, we obtain

$$E_n = E_b + [\eta\beta E_m - (2-\beta)E_b] \tag{8}$$

According Eq. 8 for freestanding nanoparticles we have (XIE, *et al*., 2004)

$$\frac{E_n}{E_b} = 1 - \frac{3}{4}\propto \tag{9}$$

For embedded nanoparticles (CAO, *et al*., 2006)

$$\frac{E_n}{E_b} = 1 - \frac{3}{8}\propto\left(1 - \eta\frac{E_m}{E_b}\right) \tag{10}$$

α denotes surface-to-volume atomic ratio, where the surface details should be noted. Supposing the shape of the nanoparticle is cubic α can be deduced as:

$$\propto = \frac{8}{n^{1/3}\pi C^{2/3}k^2} \tag{11}$$

n denote the atomic number of Nano crystals. C is the atomic number of on structure cell and K the ratio between equivalent atomic radius and lattice parameter .For Face- Centered- Cubic (FCC) , Body- Centered- Cubic (BCC) and Hexagonal Close–Packed (HCP) structures C are 4,2,2 and k are $\frac{\sqrt{2}}{4}, \frac{\sqrt{3}}{4}, \frac{1}{2}$ respectively (ASKELAND and PHULE, 2003).

Substituting Eq.11 in to Eq.9 the cohesive energy for freestanding nanoparticles we have (XIE, *et al*., 2005)

$$E_n = E_b\left(1 - \frac{6}{n^{1/3}\pi C^{2/3}k^2}\right) \tag{12}$$

We can define a shape factor μ as the ratio of two surface areas:

$$\mu = \frac{S}{S_{cubic}} \tag{13}$$

S is the surface area of particle in random shape and S_{cubic} shows the surface area of the cubic particles. The values of shape factor for nanoparticles in different shape are listed in table 1.

With combining Eqs.11 with 12 the cohesive energy of freestanding nanoparticles with random shape we can be described as:

$$\frac{E_n}{E_b} = 1 - \frac{6\mu}{n^{1/3}\pi C^{2/3}k^2} \tag{14}$$

Based on the same conception, the cohesive energy of nanoparticles under embedded condition is:

$$\frac{E_n}{E_b} = 1 - \frac{3\mu}{n^{1/3}\pi C^{2/3}k^2}\left(1 - \mu\frac{E_m}{E_b}\right) \tag{15}$$

According to relation 5, for freestanding nanoparticles we have:

$$\frac{T_{cn}}{T_{cb}} = 1 - \frac{6\mu}{n^{1/3}\pi C^{2/3} k^2} \qquad (16)$$

For embedded nanoparticles:

$$\frac{T_{cn}}{T_{cb}} = 1 - \frac{3\mu}{n^{1/3}\pi C^{2/3} k^2}\left(1 - \mu \frac{T_{CM}}{T_{Cb}}\right) \qquad (17)$$

Curie temperature function for different shape of freestanding Co, Fe, Gd, Ni, Tb nanoparticles is shown in figure 1. The Curie temperatures of ultrafine Fe, Co and Ni particles are numerically shown in Fig1.

1.2. Theory of Size Effect on Curie Temperature

In this section we study about a thermodynamics approach to the mechanism of size dependent of ferromagnetic transition temperature. This method is based on Lindeman criterion for melting Mott’s expression for the vibrational melting entropy and Shi model for the size dependent melting temperature.

It is worth emphasizing that the termination of the lattice periodicity in the surface normal has two effects. One is the reduction of the coordination numbers (CNs) of surface atoms and the other is the creation of a surface potential barrier. Both result in a large number of physical quantities $\sigma^2(D)$ at the surfaces or interfaces of nanocrystals being different from the internal counterparts$\sigma^2(D)$. Based on the mean-field approximation, the physical quantity of nanocrystals $[\sigma^2(D)]$ can be given as (Frank, 1994):

$$\sigma^2(D) = \sigma_v{}^2(D) + [\sigma_s{}^2(D) - \sigma_v{}^2(D)]\frac{n_s}{n_v} \qquad (18)$$

where the subscript *s* and *v* indicate the surface atoms and the atoms located within the Nano crystals, respectively, $n_s/n \propto 1/D$ is the ratio of the number of surface atoms (*n*s) to the total atom number (*n*) of Nano crystals(Frank, 1994). We have:

$$\frac{n_s}{n_v} = \frac{\frac{4\pi r^2 h}{V_0}}{\left[\frac{4\pi r^2}{3V_0} - \frac{4\pi r^2 h}{V_0}\right]} = \frac{3h}{r-3h} \qquad (19)$$

When the particle is spherical or quasi-spherical V_0 and h are atomic volume and diameter of a nanocrystalrespectively. With changing nomination, write the relation 19 in form $x = \frac{n_s}{n_v} = \frac{D_0}{D-D_0}$. Then we soppose:

$$\propto = \frac{\sigma_s^2(D)}{\sigma_v^2(D)} = \frac{\sigma_s^2(\infty)}{\sigma_v^2(\infty)} \qquad (20)$$

Variation of σ^2 is:

$$\sigma^2(x+dx) - \sigma^2(x) = (\propto - 1)\sigma^2(x)dx \qquad (21)$$

With the integration of relation 21, we can write:

$$\int_{\infty}^{D} \frac{d\sigma^2(x)}{\sigma^2(x)} = (\propto - 1)\int_0^x dx \qquad (22)$$

In terms of the definition of D_0 and the bulk boundary condition, two asymptotic limits should be satisfied, namely $Q(D)/Q(\infty) \to 0$, when $D \to D_0$, and $Q(D)/Q(\infty) \to 1$, when $D \to \infty$. Then we obtain:

$$\frac{\sigma^2(r)}{\sigma^2(\infty)} = exp\left((\propto -1)x\right) = exp\left((\propto -1)\frac{D_0}{D-D_0}\right) = exp\left(\frac{(\propto-1)}{(\frac{D}{D_0}-1)}\right)$$
(23)

For a nanoparticle D is its diameter, for a nanowire, D is taken as its diameter. For a film D denotes its thickness. D_0 denotes a critical size at which all atom of a low dimensional material are located on its surface. Since

$$4\pi h\left(\frac{D_0}{2}\right)^2 = \frac{4\pi}{3}\left(\frac{D_0}{2}\right)^3 \qquad D_0 = 6h \qquad d = 0$$
$$2\pi\left(\frac{D_0}{2}\right) = \pi\left(\frac{D_0}{2}\right)^2 \qquad D_0 = 4h \qquad d = 1$$
$$2\left(\frac{D_0}{2}\right) = 2h \qquad D_0 = 2h \qquad d = 2 \qquad (24)$$

Where d=0 for particles d=1 for nanorods and d=2 for thin films. In short we can conclude that:

$$D_0 = 2(3-d)h \qquad (25)$$

h is atomic diameter and d shows a dimension. Along the consideration of melting based on Lindemann's criterion, a crystal melts when the $\frac{\sigma}{H} = c$ (Lindemann, 1910). C is a parameter which depends on crystal structure. *H* is assumed to be a size-independent constant. If suppose that $\sigma^2(D,T) = f(D)T$, at temperatures close to the melting temperature we have:

$$\frac{\sigma^2(D,T)}{\sigma^2(\infty,T)} = \frac{f(D)}{f(\infty)} \qquad (26)$$

When $= T_m(D)$, we can write:

$$\frac{f(D)}{f(\infty)} = \frac{\{\frac{\sigma^2[D,T_m(D)]}{h^2}\}}{\{\frac{\sigma^2[\infty,T_m(\infty)]}{h^2}\}}\left[\frac{T_m(\infty)}{T_m(D)}\right] = \frac{T_m(\infty)}{T_m(D)} \qquad (27)$$

With regard to relations 23, 26 and 27, the result is:

$$\frac{T_m(D)}{T_m(\infty)} = \frac{\sigma^2(\infty)}{\sigma^2(D)} = exp\left(\frac{-(\propto-1)}{(\frac{D}{D_0}-1)}\right) \qquad (28)$$

The modern form of Lindemann's criterion has been given by

$$\theta_D^2(\infty) = f[\frac{T_m(\infty)}{\left(MV^{\frac{2}{3}}\right)}]^{\frac{1}{2}} \qquad (29)$$

Where *f* denotes a fraction of the nearest-neighbor spacing at which melting occurs, *M* is the molecular weight, and *V* is the molar volume. Size dependence of the function of nanocrystals can be obtained as a generalization of the above relationship (Jiang, *et al.*, 1998)

$$\frac{T_m(D)}{T_m(\infty)} = \frac{\theta_D^2(D)}{\theta_D^2(\infty)} \qquad (30)$$

$$\frac{T_m(D)}{T_m(\infty)} = \frac{\theta_D^2(D)}{\theta_D^2(\infty)} = exp\left(\frac{-(\propto-1)}{(\frac{D}{D_0}-1)}\right) \qquad (31)$$

Using the mean field approximation, we have this relation:

$$K_B T_{cm}(\infty) = E_{exc}(\infty) \qquad (32)$$

$E_{exc}(\infty)$ is the The average energy of thermal vibrations that is related to T in this form:

$$m(2\pi\vartheta_E)^2 = \sigma^2(T) = K_B T \qquad (33)$$

ϑ_E is Einstein frequency and m is atomic mass. At $T = T_{cm}(\infty)$ we have:

$$m(2\pi\vartheta_E)^2 = \sigma^2(T_{cm}(\infty)) = K_B T_{cm}(\infty) \qquad (34)$$

As a result we can write $\sigma^2 \propto T_{cm}(\infty)$. So Curie temperature is obtained:

$$\frac{T_{cm}(D)}{T_{cm}(\infty)} = \frac{\theta_D^2(D)}{\theta_D^2(\infty)} = exp\left(\frac{-(\alpha-1)}{(\frac{D}{D_0}-1)}\right) \qquad (35)$$

This is the relation of ferromagnetic nanoparticle Curie temperature and its size. This relation for five elements is shown in figure 7. For a nanocrystal with free surface or one deposited on inert substrate, α has been determined by Mott's consideration (Zhao, *et al.*, 2001) and (Jiang, *et al.*, 1999):

$$\alpha = \frac{1+2s_{vib}(\infty)}{3R} \qquad (36)$$

To prove this relationship, use Mott's expression vibrational melting entropy in a bulk crystal:

$$s_{vib}(\infty) = (\frac{3k}{2})\ln\{T_m(\infty)\times[C_s(\infty)/C_l(\infty)]^2 [\pi^4/(6N_0)]^3/M \qquad (37)$$

Where $C_s(\infty)$ and $C_l(\infty)$ are ultrasound propagation velocities of the bulk liquid and the bulk crystal, respectively. Since $C_s(r)/C_l(r) \approx C_s(\infty)/S_l(\infty)$ we obtain:

$$S_{vib}(r) - S_{vib}(\infty) = \frac{3k}{2}\ln(\frac{T_m(r)}{T_m(\infty)}) \qquad (38)$$

According to Eq. 31 we have:

$$S_{vib}(r) = S_{vib}(\infty) - (\frac{3k}{2}[\frac{(\alpha-1)}{\frac{r}{r_0}-1}]) \qquad (39)$$

Melting entropy S_m consists of three contributions. Positional vibrational S_{pos} and electronic component S_{el}. S_m is the essential contribution to for metals and other terms are small. Then we can conclude that:

$$S_m(r) = S_m(\infty) - (\frac{3k}{2}[\frac{(\alpha-1)}{\frac{r}{r_0}-1}]) \qquad (40)$$

If supposed boundary condition $r \longrightarrow 2r_0$, $S_m(r) \to 0$, we obtain eq 36.

2. Numerical Calculation

In Figures 1a, 1b, 1c, 1d and 1f, transition temperature is plotted versus atomic number for different geometrical shape of freestanding Co, Fe, Ni, Gd and Tb nanoparticles according to equation 16. As you can see, for all five elements, the diagram varations is as exponential function. Sphere and decahedron has the highest and the lowest transition temperature, respectively. As you can see these diagrams have the same trend for the five ferromagnetic elements. In these pictures observed that Curie temperature difference can be caused by different geometric shapes. This effect is evident in Less than ten nanometers. Shape factor value of for some structure of nanoparticles is shown in table 1.

In Placement nanoparticle systems, Curie temperature depends on the interaction between the particle and the substrate. When there are weak interactions at the surface, localized particles behave as free particles and The Curie temperature decreases with decreasing size. In the other hand when there are strong interactions, Curie temperature nanoparticles can be localized through conflicting changes.

Table-1. Shape factor value of for some structure of nanoparticles.

Shape	μ
cube	**1**
sphere	**0.8060**
octahedron	**0.9532**
decahedron	**1.0110**

In figure 2 the Curie temperature function (Eq 16) for nanoparticles of Fe, Co, Ni, Gd and Tb and has been compared. The shape factor value is considered one, Hence the shape is cube. In this picture, the function varies exponentially. As you see in this figure, varations of Co and Tb is more and less, respectively. We find that for ferromagnetism with higher Curie temperature , Slope varations is more and The opposite is also true. In Co and Fe nanoferromagnetic, Curie temperature variations is higher than other elements. As described earlier the size varations will effect the Curie temperature.

Fig-1. Comparisons of Curie temperature function for different shape of freestanding nanoparticles.(a) Co.(b) Fe.(c) Ni. (d) Gd. (f) Tb.

(a)

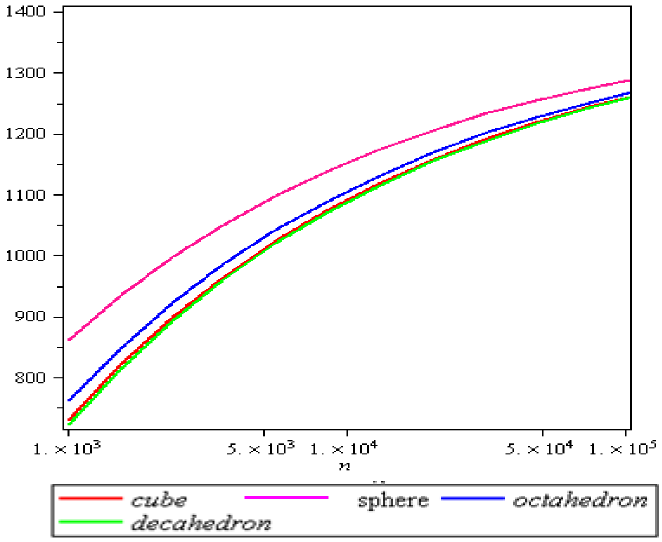

(b)

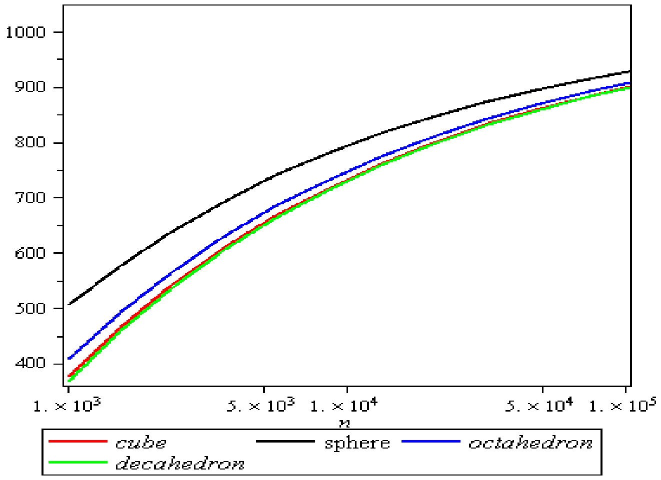

(c)

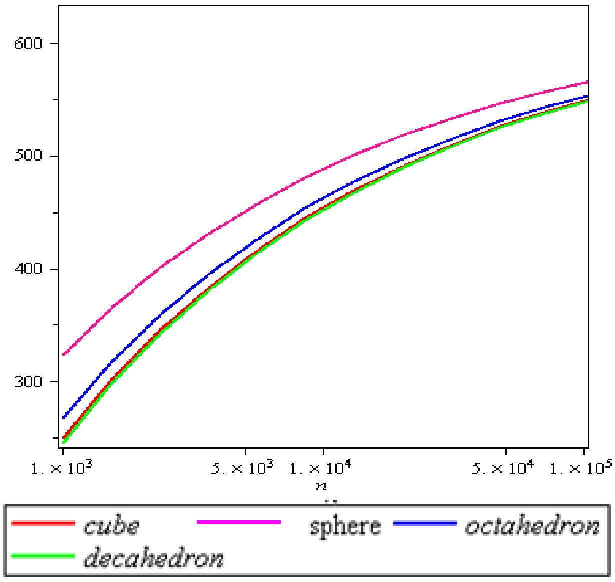
600
500
400
300
1. × 10³
5. × 10³
1. × 10⁴
5. × 10⁴
1. × 10⁵
n
cube
sphere
octahedron
decahedron

(d)

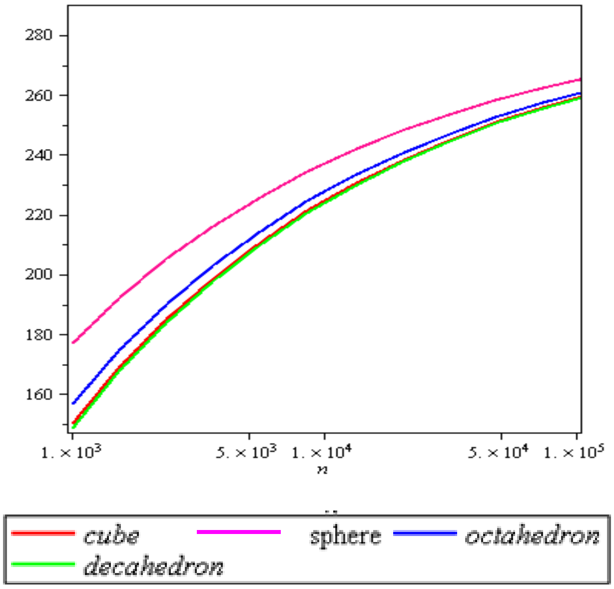
280
260
240
220
200
180
160
1. × 10³
5. × 10³
1. × 10⁴
5. × 10⁴
1. × 10⁵
n
cube
sphere
octahedron
decahedron

(f)

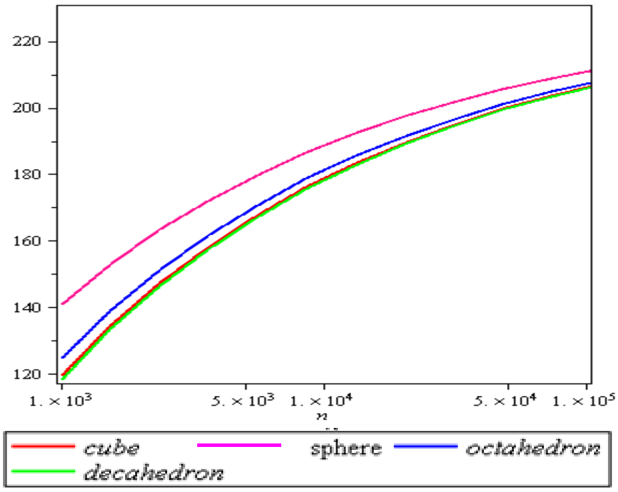
220
200
180
160
140
120
1. × 10³
5. × 10³
1. × 10⁴
5. × 10⁴
1. × 10⁵
n
cube
sphere
octahedron
decahedron

In figure 3 curie Temperature varations is plotted for 5 nanomagnetics according to Eq 35 and for Fe, Co, Ni, Gd and Tb nanoparticles Comparison is done.

According to Eqs (35) and (31), if α > 1, then $T_c(D)$decrease with decreasing *D*. when α < 1, $T_c(D)$ increase with decreasing *D*. As observed in this figure, while reducing the size, Curie temperature is reduced.

To compare the different types of nanocrystals, we use the 3d plot diagram. In Figure 4, Curie temperature function (equation 35) is plotted as a three-dimensional.In this figure, Function $T_c(D)$ versus D and d. As you study before d Determines that the nanocrystal is nanoparticle, nanorod or thin film. By Using the plot 2d we can Analysis the plot 3d.

In figure 5 you can see 3 graphs. One is for nanoparticles(d=0), the other is for nanorods (d=1) and d=3 for thin films. From this figure, We can find that. Namely the curie temperature of nanoparticle drops more than the others. This can be explained that Contact surface of nanoparticle with the environment is more than the others.

Fig-2. Comparison of Curie temperature function (Eq 16) for freestanding nanoparticles Fe, Ni, Gd, Co and Tb with μ = 1

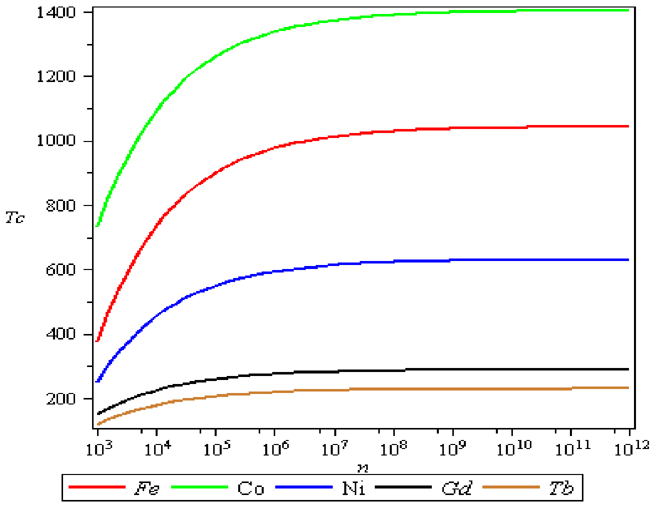

Fig-3. Comparison of Curie temperature function (Eq 35) for freestanding nanoparticles Fe, Ni, Gd, Co and Tb.

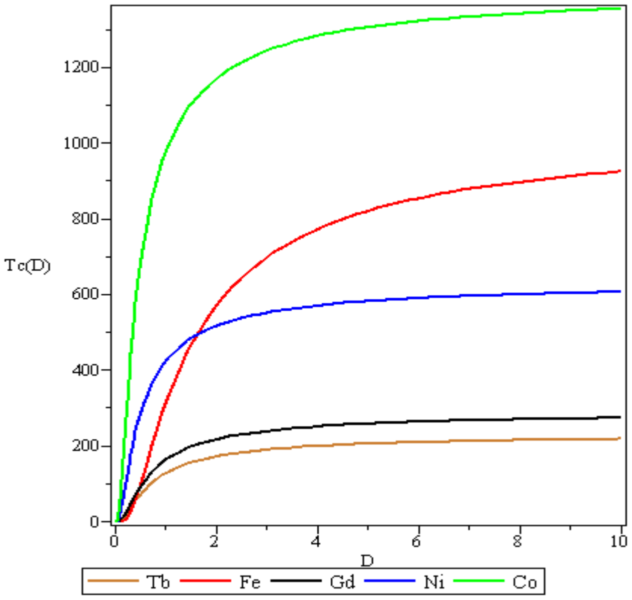

At the figure 6a, 6b and 6c can also see the diagrams of relations 5 , 35 and experimental results for ferromagnetism of Fe, Ni and Co. We can say that when the particle size decreases, the Curie temperature is decrease too. But the relation 5 is more consistent with the experimental results. To better understand this see the table 2,3,4.

table 2 shows the average percentage error of relation 35 and 5 with experimental results for Fe ferromagnetic that is 19% and 44%, respectively.

Table 3 numerical values for thin layers of Ni ferromagnetic. we will find that the relation 35 is more agreement with experimental data . percent error of relations 35 and 5 with the experimental data are 11% and 28%, respectively. These results suggest that the relation 35 is closer to the truth.

Also If you consider to the table 4 can see percent error of relations 35 and 5 are 22% and 56%,respectively. In general it can conclude that the relation 35 is more functional than the relation 5.

Fig-4. Three dimensional plot of the function $T_c(D)$ versus D(nm) and d(nm). (Eq35)

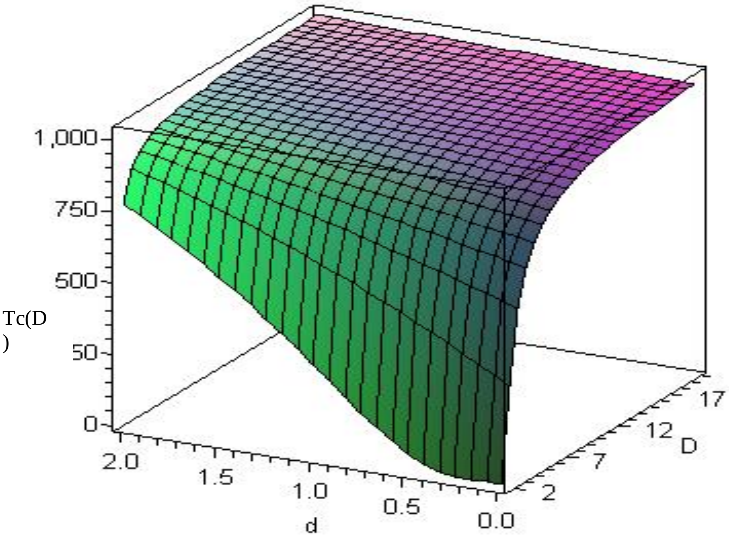

Fig-5. The corresponding contour plot of figure 8.

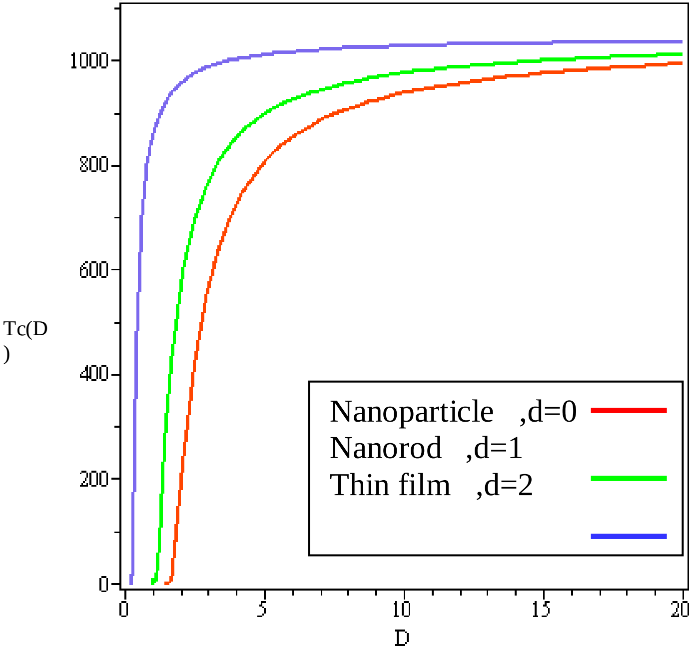

Fig-6. Comparison the relations 35 and 5 with the experimental results. (a) for ferromagnetic Fe thin film (b) For Ni thin film (c) For Co thin film (YANG and JIANG, 2005)

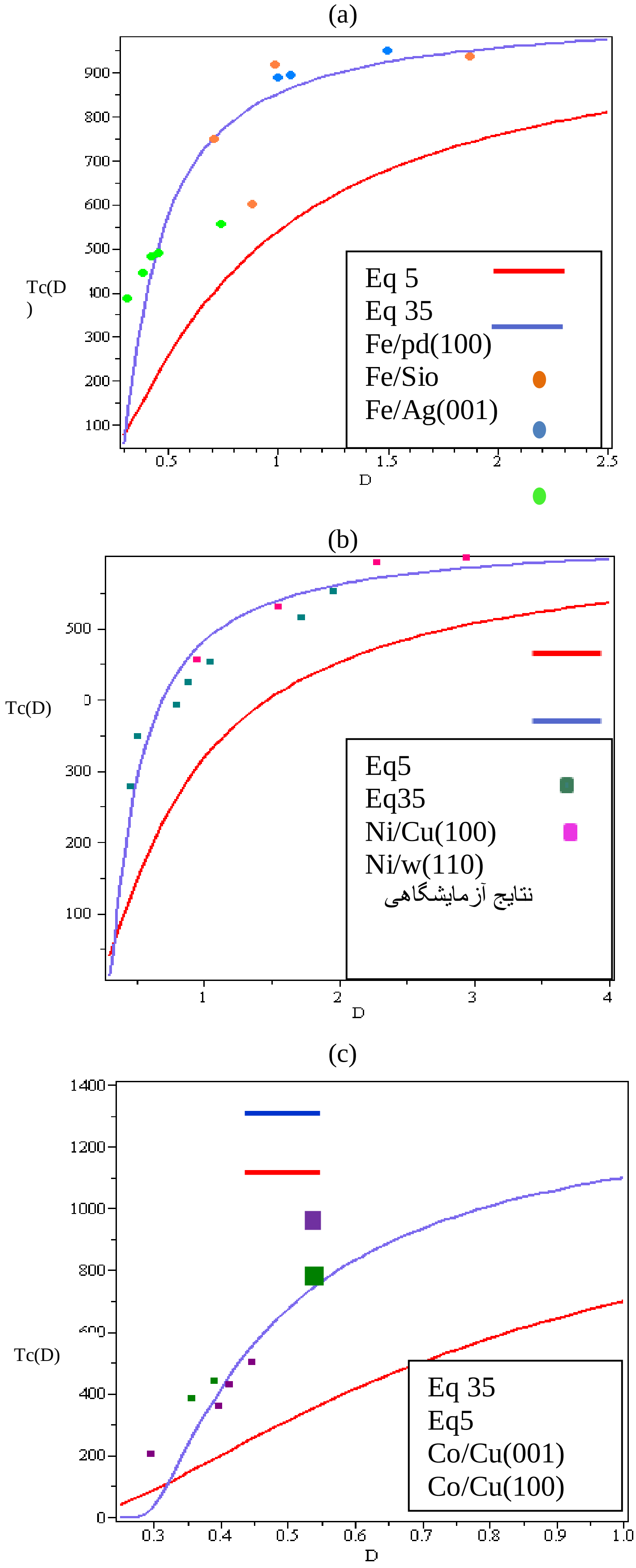

Fig 9

Table-2. Numerical values obtained from the relation 35 and 5 and Percent error of the relations compared with experimental for Fe thin film (YANG and JIANG, 2005)

	D (nm)	Film's kind	$T_c(D)$ $Th1$	$T_c(D)$ $Th2$	$T_c(D)$ Ex	Percent error of relations 35 compared with experimental results	Percent error of relations 5 compared with experimental results
1	0.30	Fe/pd(100)	121.88	75.00	392.50	67%	81%
2	0.40	Fe/pd(100)	378.12	168.75	450.00	16%	62%
3	0.44	Fe/pd(100)	468.75	240.62	475.00	1%	49%
4	0.50	Fe/pd(100)	575.00	256.25	487.00	18%	47%
5	0.75	Fe/pd(100)	765.62	418.75	550.00	39%	24%
6	0.75	Fe/Sio	771.88	425.00	900.00	14%	52%
7	1.00	Fe/Sio	846.88	540.62	900.00	5%	40%
8	1.50	Fe/Sio	921.77	675.00	960.00	3%	30%
9	0.66	Fe/Ag(001)	725.00	362.50	750.00	2%	51%
10	0.90	Fe/Ag(001)	825.00	500.00	600.00	39%	16%
11	1.00	Fe/Ag(001)	850.00	534.00	1025.00	17%	47%
12	2.05	Fe/Ag(001)	954.00	765.63	1025.00	6%	25%
		Average percent				**19%**	**44%**

Table-3. Numerical values obtained from the relation 35 and 5 and Percent error of the relations compared with experimental for Ni thin film (YANG and JIANG, 2005)

	D(nm)	Film's kind	$T_c(D)$ $Th1$	$T_c(D)$ $Th2$	$T_c(D)$ Ex	Percent error of relations 35 compared with experimental results	Percent error of relations 5 compared with experimental results
1	0.4	Ni/Cu(100)	167.36	96.48	280	40%	65%
2	0.5	Ni/Cu(100)	290.31	144.21	350	17%	59%
3	0.8	Ni/Cu(100)	434.00	262.82	390	11%	32%
4	1.0	Ni/Cu(100)	485.58	316.34	420	16%	25%
5	1.0	Ni/w(110)	485.58	316.34	450	7%	30%
6	1.2	Ni/Cu(100)	508.73	359.74	450	13%	20%
7	1.5	Ni/w(110)	534.00	406.03	520	2%	22%
8	1.8	Ni/Cu(100)	555.00	434.96	500	11%	13%
9	2.0	Ni/Cu(100)	559.00	452.31	540	3%	16%
10	2.0	Ni/w(110)	559.00	452.31	550	1%	18%
11	2.2	Ni/w(110)	566.58	468.22	590	3%	21%
12	2.8	Ni/w(110)	581.05	497.15	600	3%	17%
		Average percent				**11%**	**28%**

Table-4 . Numerical values obtained from the relation 35 and 5 and Percent error of the relations compared with experimental for Co thin film (YANG and JIANG, 2005)

	D	Film's kind	$T_c(D)$ $Th1$	$T_c(D)$ $Th2$	$T_c(D)$ Ex	Percent error of relations 35 compared with experimental results	Percent error of relations 5 compared with experimental results
1	0.35	Co/Cu(100)	238.27	93.92	390.00	38%	76%

2	0.39	Co/Cu(100)	374.06	193.89	440.00	15%	56%
3	0.30	Co/Cu(001)	95.00	80.00	200.00	52%	60%
4	0.40	Co/Cu(001)	408.71	196.53	370.00	10%	47%
5	0.41	Co/Cu(001)	443.49	215.66	460.00	3%	53%
6	0.47	Co/Cu(001)	600.00	283.49	500.00	17%	43%
Average percent						**22%**	**56%**

3. Conclusions

The shape or size of nanoparticles also plays an important role on the critical temperature variation within a quite ultrafine size range. For this reason two simplified model is developed for the size and shape dependent Curie temperature of ferromagnetic nanoparticles. These models predicts a decrease of Curie temperature with decreasing size or shape of ferromagnetic nanocrystals.When considering the curie temperature variations to the structure we can see that sphere and decahedron geometry has the highest and the lowest curie temperature, respectively. Also we conclude that co and Tb has the most and the least curie temperature variations respect to the both size and structre, respectively.

In general it can be said that at the nanoscale, phase transition occurs at a lower temperature. Also decreasing of curie temperature nanoparticle is more than the thin films and nanorods.

Also we saw that All calculations of shape and size dependent of Curie temperature are consistent with the theoretical results and According to the tables there is slightly different between the theoretical results and the available experimental results and we would consider to carried out more experiments in this field in future.

References

Adamson, A. W., (1990). Physical chemistry of surface. New York: John-Wiley & Sons Inc.

Askeland, D. R. and Phule, P. P., (2003). The science and engineering of materials. New York: Thomson Learning Inc. pp: 84.

Cui, X. F., Zhao, M. and Jiang, Q., (2005). Curie transition temperature offerromagnetic low-dimensional metals. [J], Thin Solid Films, 472(1/2): 328−333.

Cao, L. F., Xu, G. Y., Xie, D., Guo, M. X., Luo, L., Li, Z. and Wang, M. P., (2006). Thermal stability of Fe, Co, Ni metal nanoparticles. [J], Phys Status Solid (B), 243: 2745−2755.

Evans, R., Nowak, U., Dorfbaner, F., Shrefl, T., Mryasov, O., Chantrell, R. W. and Grochola, G., (2006). The influence of shape andstructure on the Curie temperature of Fe and Co nanoparticles. [J], J. Appl.Phys., 99: 08G703−1−3.

Fisher, M. E. and Barber, M. N., (1972). Scaling theory for finite-size effects in the critical region. [J], Phys Rev Lett, 28: 1516−1519.

Frank, G. Shi., (1994). Size dependent thermal vibrations and melting in nanocrystals. Journal of Materials Research, 9: 1307-1314. Doi:10.1557/JMR.1994.1307.

Hong, W. H., Sun, C. Q., Li, S., Bai, H. L. and Jiang, E. Y., (2005). Impact of bond-order loss on surface and nanosolid magnetism. [J], Acta Mater, 53(11): 3207−3214.

Jiang, Q., Tong, H.Y., Hsu, D.T., Okuyama K. and Shi, F. G., (1998). Thermal stability of crystalline thin films. Thin Solid Films, 312: 357.

Jiang, Q., Shi, H.X. and Zhao, M., (1999). Melting thermodynamics of organic nanocrystals. J. Chem. Phys, 111: 2176.

Lindemann, F. A., (1910). Z. Phys., 11: 609.

Nikolaev, V. I. and Shipilin, A. M., (2003). The influence of breaking of exchange bonds on the curie temperature. [J], Phys Solid State, 45: 1079−1080.

Sun, C. Q., Zhong, W. H., Li, S., Tay, B. K., Bai, H. L. and Jiang, E. Y., (2004). Coordination imperfection suppressed phase stability of ferromagnetic, ferroelectric, and superconductive nanosolids. [J], JPhysChem B, 108(3): 1080−1084.

Tang, N. J., Zhong, W., Jiang, H. Y., Wu, X. L., Liu, W. and Du, Y. W., (2004). Nanostructured magnetite (Fe3O4) thin films prepared by sol-gel method. [J], J Magn Mater, 282: 92−95.

Wautelet, M., Dauchot, J. P. and Hecq, M., (2003). On the phase diagram of non-spherical nanoparticles. [J], J Phys Condens Matt, 15: 3651−3655.

Xie, D., QI, W. H. and Wang, M. P., (2004). Size and shape dependent melting-thermodynamic properties of metallic nanoparticles. [J], ActaMetall Sin, 40(10): 1041−1044, (In Chinese)

Xie, D., Wang, M. P. and Qi, W. H., (2004). A simplified model to calculate the surface-to-volume atomic ratio dependent cohesive energy of nanocrystals. [J], J. Phys. Condense Mater, 16: L401−L405.

Xie, Dan., Wang, Ming-Pu. and Cao, Ling-Fei., (2005). A simplified model to calculate the higher surface energy of free-standing nanocrystals. [J], Phys Status Solid (B), 242(8): R76−R78.

Yang, C. C. and Jiang, Q., (2005). Size and interface effects on critical temperatures of ferromagnetic, ferroelectric and superconductive nanocrystals. [J], Acta Mater, 53(11): 3305−3311.

Zhang, R. J. and Willis, R. F., (2001). Phys. Rev. Lett., 86: 2665

Zhao, M. X., Zhou, H. and Jiang, Q., (2001). Comparison of different models for melting point change of metallic Nano crystals J. Mater. Res., 16: 3304.